AMB Express

ORIGINAL ARTICLE Open Access

Metabolic engineering of *Parageobacillus thermoglucosidasius* for thermophilic production of 1-butanol

Pablo Doménech[1,2], Ivan Pogrebnyakov[1], Sheila Ingemann Jensen[1], Jasper L. S. P. Driessen[1], Anders Riisager[2] and Alex Toftgaard Nielsen[1*]

Abstract

1-Butanol is a promising compound for the ongoing green transition due to its potential both as a fuel and as a platform chemical, serving as a common intermediate for the bulk production of other valuable products. In this study, the thermophilic bacterium *Parageobacillus thermoglucosidasius* DSM 2542 was engineered to produce 1-butanol by introducing a butanol-producing pathway with thermostable enzyme variations derived from various thermophilic microorganisms. To achieve successful metabolic engineering, the relevant genes were inserted into two different chromosomal locations, employing both constitutive and inducible promoter systems. The resulting strains exhibited varying 1-butanol production depending on the promoter system used for the first half of the genes, with titres reaching up to 0.4 g/L when working under oxygen-limiting conditions. This serves as a foundation for further metabolic optimization to utilize the strain under industrial conditions.

Keywords Butanol, *Parageobacillus thermoglucosidasius*, Thermophilic fermentation, Metabolic engineering

Introduction

The current energy crisis along with the need to limit industrial CO_2 emissions is forcing us to find alternative fuels that can replace traditional ones with a non-renewable fossil origin. Biofuels, obtained sustainably from renewable resources like biomass, hold the potential for making a partial replacement possible. Fermentation of the carbohydrates present in biomass enables the production of several compounds, which can be utilised as biofuels—(bio)ethanol being the most widespread. Over the last years, 1-butanol (also known as n-butanol, onwards referred to as simply butanol) has attracted attention as a better biofuel than ethanol, given its higher energy content, lower vapour pressure and solubility in water, and better compatibility with existing infrastructures due to its closer similarity to conventional gasoline (Nahreen and Gupta 2013; Fletcher et al. 2016; Trindade and dos Santos 2017).

Butanol is a four-carbon primary alcohol that has several uses other than its potential as a fuel, namely as a solvent or as a bulk chemical. It can be chemically upgraded to commodity chemicals such as butyl acrylate or butyl methacrylate (Ndaba et al. 2015) or even jet fuels when combined with other organic compounds (Anbarasan et al. 2012; Doménech et al. 2022). Butanol has been traditionally produced by the bacteria *Clostridium acetobutylicum* in the ABE (acetone-butanol-ethanol) fermentation process, where it is the main product (Weizmann 1919;

*Correspondence:
Alex Toftgaard Nielsen
atn@biosustain.dtu.dk
[1]The Novo Nordisk Foundation Center for Biosustainability, Technical University of Denmark, Søltofts Plads 220, 2800 Kgs. Lyngby, Denmark
[2]Department of Chemistry, Centre for Catalysis and Sustainable Chemistry, Technical University of Denmark, Kemitorvet 207, 2800 Kgs. Lyngby, Denmark

Nguyen et al. 2018). Nowadays, industrial production of butanol is mostly carried out by chemical catalysis starting from fossil-based resources via the oxo-process, where propene is hydroformylated with syngas (CO/H_2) to butanal, which is then hydrogenated to obtain the primary alcohol (Xue et al. 2017). Butanol can also be chemically obtained from renewable sources, such as biomass-derived ethanol, by self-condensation (Guerbet reaction) of the two-carbon alcohol with itself (Gabriëls et al. 2015; Ndaba et al. 2015).

Replacement of ABE fermentation by other means for butanol production has largely occurred due to the technical and economic leverages petroleum-based refineries have over bio-based processes (Breitkreuz et al. 2014; Nguyen et al. 2018). However, environmental concerns are presently the main driver towards finding solutions that are both sustainable and competitive. Thermophilic fermentation (carried out at 45–70 °C), as opposed to traditional mesophilic fermentation (20–45 °C), shows sufficient advantages when considering its application at an industrial scale. Working at higher temperatures allows for faster kinetics, decreased risk of contamination and therefore reduced sterility requirements, and decreased cooling cost as fermentations are exothermic processes (Loder et al. 2015; Pogrebnyakov et al. 2017; Sheng et al. 2023). Moreover, if the fermentation is to be implemented within a 2nd generation biorefinery, simultaneous saccharification and fermentation (SSF) could be performed, where the fermentation step can be integrated with the prior saccharification step (typically run at 50 °C) due to the similar working temperatures of both processes. The final benefit widely addressed is the possibility of in-situ product recovery (ISPR) when aiming to obtain volatile compounds, that could get evaporated as they are produced when working at sufficiently high temperatures—this is the case of acetone (Zeldes et al. 2018) or ethanol (Abdel-Banat et al. 2010). While butanol has a high boiling point of 117.6 °C (91.4 °C when considering its azeotrope with water) (Luyben 2008; Rumble 2022), the increased vapour pressure when working at high temperatures still allows for a reduced product concentration that would alleviate inhibition on the cell factory (Gorter de Vries et al. 2024). Despite these advantages, reports on thermophilic butanol production are scarce, with published works solely addressing its engineering in xylose-consuming *Thermoanaerobacterium* species (Bhandiwad et al. 2014; Jiang et al. 2018).

Advances in biobutanol production mostly focus on the engineering of *C. acetobutylicum*, an industrial cell factory which works at mesophilic conditions. The introduction of butanol-production pathways has also been successfully introduced to other industrially viable mesophilic non-native hosts, namely *Escherichia coli* (Atsumi et al. 2008) and *Saccharomyces cerevisiae* (Swidah et al. 2018), thoroughly reviewed by Nawab et al. (2020). As for thermophiles, one possible host with great potential to be utilised for heterologous pathways is *Parageobacillus thermoglucosidasius* (formerly *Geobacillus thermoglucosidasius*). This gram-positive bacterium has had some recent developments for its genetic modification, notably the development of promoter and RBS libraries (Pogrebnyakov et al. 2017), several synthetic biology tools in the form of specific shuttle vectors (Kananavičiūtė and Čitavičius 2015; Madika et al. 2022; Millgaard et al. 2023) and the implementation of CRISPR/Cas9 (Lau et al. 2021). *P. thermoglucosidasius* has been successfully engineered for the production of acetone (Pogrebnyakov and Nielsen 2022), ethanol (Cripps et al. 2009) and butanediol (Zhou et al. 2020; Sheng et al. 2023) among others, but so far not to produce butanol. The aim of the current work was therefore to engineer the strain for the thermophilic production of butanol, by employing existing tools previously developed for the microorganism.

Heterologous pathways for the fermentative production of butanol are typically based on the natural pathway present in *C. acetobutylicum* (Fig. 1). Starting from two molecules of acetyl-CoA, this consists of a six-step enzymatic cascade, where electrons are obtained in the form of up to four NADH equivalents for each molecule of produced butanol.

Loder et al. (2015) developed a hybrid synthetic pathway to produce butanol from acetyl-CoA using thermostable variations of the original pathway enzymes, aiming also for an enhanced selectivity towards butanol as opposed to ethanol. Genes *thl*, *hbd* and *crt* were initially sourced from *Caldanaerobacter subterraneus* subsp. *tengcongensis*, *ter* came from *Spirochaeta thermophila*, and *bad* and *bdh* originated from *Thermoanaerobacter* sp.; all of them with optimal growth temperatures between 60 and 75 °C. The set of enzymes synthesised from these genes was the starting point for

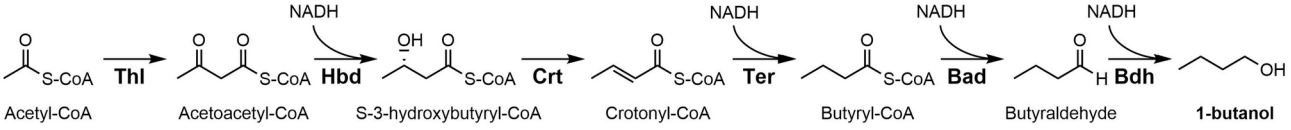

Fig. 1 Simplified metabolic pathway for the production of 1-butanol starting from acetyl-CoA (Loder et al. 2015; Foulquier et al. 2022). Thl: thiolase; Hbd: 3-hydroxybutyryl-CoA dehydrogenase; Crt: 3-hydroxybutyryl-CoA dehydratase; Ter: trans-2-enoyl-CoA reductase; Bad: aldehyde dehydrogenase; Bdh: alcohol dehydrogenase

the present work—the genes responsible for the expression of each enzyme were inserted into a wild-type strain of *P. thermoglucosidasius* DSM 2542. Different strategies for the pathway insertion were pursued, including the study of different promoters, as well as different small-scale fermentation configurations, aiming for an enhanced butanol production and efficient microbial performance.

Materials and methods

Strains, plasmids and media

All chemicals were obtained from Sigma Aldrich-Merck (St. Louis, USA), ThermoFisher Scientific (Waltham, USA) or VWR (Radnor, USA) and used as received. The different strains and plasmids (obtained or constructed) used are compiled in Table 1.

E. coli cells were grown in lysogeny broth (LB) medium at 250 rpm or LB agar, whenever required. For strain construction, *P. thermoglucosidasius* was grown in SPY medium containing 16 g/L soy peptone, 10 g/L yeast extract, and 5 g/L NaCl; or trypticase soy agar (TSA) plates (BD Biosciences, USA). Cells were prepared for transformation using electroporation (EP) buffer, containing 0.5 mol/L mannitol, 0.5 mol/L sorbitol, and 10 vol% glycerol. When selecting for antibiotic resistance, media was supplemented with kanamycin (Kan): 6.25 µg/mL for *E. coli* and 12.5 µg/mL for *P. thermoglucosidasius*. Unless otherwise stated, *E. coli* was grown at 37 °C and *P. thermoglucosidasius* was grown at 60 °C.

Performance of the constructed cells was assessed in thermophile minimal medium (TMM), adapted from Fong et al. (2006). TMM contained, per litre: 930 mL of Six salts solution (consisting of 4.6 g NaCl, 1.35 g Na_2SO_4, 0.23 g KCl, 0.037 g KBr, 1.72 $MgCl_2{\cdot}6H_2O$ and 0.83 g $NaNO_3$), 50 mL of 1 M 4-Morpholinepropanesulfonic acid (MOPS) solution, 10 mL of 1 mM $FeSO_4$ in 0.4 M tricine, 10 mL of 0.132 M K_2HPO_4, 10 mL of 0.953 M NH_4Cl, 0.5 mL of 1 M $CaCl_2$, 0.5 mL of trace elements solution (consisting of 1 g $FeCl_3{\cdot}6H_2O$, 0.18 g $ZnSO_4{\cdot}7H_2O$, 0.12 g $CuCl_2{\cdot}2H_2O$, 0.12 g $MnSO_4{\cdot}H_2O$ and 0.18 g $CoCl_2{\cdot}6H_2O$; per litre), and 1 mL of 1000x Wolfe's vitamin solution (consisting of 10 mg pyridoxine HCl, 5 mg thiamine HCl, 5 mg riboflavin, 5 mg nicotinic acid, 5 mg Ca-D-(+)-pantothenate, 5 mg p-aminobenzoic acid, 5 mg thioctic acid, 2 mg biotin, 2 mg folic acid and 0.1 mg vitamin B12; per litre). TMM was supplemented, when required, with the desired carbon source and/or yeast extract (YE): unless otherwise stated, amounts used were 10 g/L glucose and 5 g/L YE.

EP buffer and SPY medium were filter sterilised; LB was autoclaved. Sterile TMM was obtained by autoclaving all salt solutions and filter-sterilising the rest of the components of the mixture independently, followed by mixing all components under aseptic conditions.

Table 1 List of strains and plasmids utilised in this work

Strain	Description	Source
P. thermoglucosidasius DSM 2542	Wild type (WT).	Bacillus Genetic Stock Center (USA)
P. thermoglucosidasius Btb-Ptet	Butanol-producing modified strain with two aTc-inducible Ptet promoter systems: Δ*ldh*::(Ptet-*thl-hbd-crt*) Δ*acx*::(*tetR*-Ptet-*ter-bad-bdh*) Δ*adh*.	This work
P. thermoglucosidasius Btb-Ptet Δ*spo0A*	Sporulation-deficient butanol-producing strain described above.	This work
P. thermoglucosidasius Btb-P10	Butanol-producing modified strain with a constitutive PgroES constitutive promoter and an aTc inducible Ptet promoter: Δ*ldh*::(PgroES_P10-*thl-hbd-crt*) Δ*acx*::(*tetR*-Ptet-*ter-bad-bdh*) Δ*adh*.	This work
P. thermoglucosidasius Btb-P13	Butanol-producing modified strain with a constitutive PgroES constitutive promoter and an aTc inducible Ptet promoter: Δ*ldh*::(PgroES_P13-*thl-hbd-crt*) Δ*acx*::(*tetR*-Ptet-*ter-bad-bdh*) Δ*adh*.	This work
P. thermoglucosidasius Btb-P15	Butanol-producing modified strain with a constitutive PgroES constitutive promoter and an aTc inducible Ptet promoter: Δ*ldh*::(PgroES_P15-*thl-hbd-crt*) Δ*acx*::(*tetR*-Ptet-*ter-bad-bdh*) Δ*adh*.	This work
Escherichia coli DH5α	F- Φ80*lacZ*ΔM15 Δ(*lacZYA-argF*) U169 *recA1 endA1 hsdR17*(rk-, mk +) *phoA supE44 thi-1 gyrA96 relA1* λ-. Utilised for plasmid construction.	ThermoFisher Scientific
Plasmid	**Description**	**Source**
pMTL61110	*E. coli/P. thermoglucosidasius* shuttle vector, pNW33N origin of replication, thermosensitive replicon, kan^R, *sfGFP*. Primarily used as backbone for plasmid construction.	(Sheng et al. 2017)
pBUT01	Full operon (*thl-hbd-crt-ter-bad-bdh*) for integration into *ldh* in *P. thermoglucosidasius*.	This work
pBUT05	Half operon (*thl-hbd-crt*) for integration into *ldh* in *P. thermoglucosidasius*.	This work
pBUT07	Half operon (*ter-bad-bdh*); left flank *crt* and right flank *ldh* in *P. thermoglucosidasius*.	This work
pBUT17	Inducible Ptet promoter with *tetR* repressor, half operon (*ter-bad-bdh*) for integration into *acx* in *P. thermoglucosidasius*.	This work
pBUT22	Inducible Ptet promoter, left flank *ldh* in *P. thermoglucosidasius* and right flank *thl*.	This work
pBUT28	Half operon (*thl-hbd-crt*, different *thl* variant) for integration into *ldh* in *P. thermoglucosidasius*.	This work
pJD45	Deletion of *adh* operon in *P. thermoglucosidasius*.	This work
P10-Slip_0880_500	Constitutive PgroES promoter P10 (Pogrebnyakov et al. 2017); left flank *ldh* in *P. thermoglucosidasius* and right flank *thl*.	Previous work, publication pending

Table 1 (continued)

Plasmid	Description	Source
P13-Slip_0880_500	Constitutive PgroES promoter P13 (Pogrebnyakov et al. 2017); left flank *ldh* in *P. thermoglucosidasius* and right flank *thl*.	Previous work, publication pending
P15-Slip_0880_500	Constitutive PgroES promoter P15 (Pogrebnyakov et al. 2017); left flank *ldh* in *P. thermoglucosidasius* and right flank *thl*.	Previous work, publication pending
pMM7	Deletion of *spo0A* in *P. thermoglucosidasius* for sporulation-deficient strains.	(Millgaard et al. 2023)

Plasmid and strain constructions

Primers were obtained from Integrated DNA Technologies (Coralville, USA), DNA constructs were obtained from Twist Bioscience (San Francisco, USA), and whole genomic DNA were obtained from DSMZ (Braunschweig, Germany). DNA fragments were amplified with the Phusion U Hot Start DNA Polymerase (ThermoFisher Scientific, Waltham, USA) with annealing temperatures of 60 °C and elongation times of 1 min per kb. Assembly of plasmid fragments was performed by uracil-specific excision reagent (USER) assisted cloning (New England Biolabs, USA), using fragments previously amplified with uracil-containing primers for their desired assembly. Plasmid cloning was performed by chemically competent *E. coli* cells. Plasmids were verified by colony PCR using OneTaq 2x Master Mix (New England Biolabs, Ipswich, USA) and the plasmids were extracted using the NucleoSpin Plasmid kit (Macherey-Nagel, Düren, Germany) and subsequently sequenced (Eurofins Genomics, Ebersberg, Germany).

Plasmid DNA (2.5 µL) were transformed into electrocompetent *P. thermoglucosidasius* cells (60 µL) by electroporation with an exponential pulse, voltage of 2.5 kV, capacitance of 10 µF and resistance of 600 Ω. Transformed cells were recovered in SPY medium for 3–4 h at 52 °C and 200 rpm, after which they were transferred to TSA plates with kanamycin and grown overnight at 52 °C. Positive transformation was checked by identifying green-fluorescent colonies, resulting from the *sfGFP* gene present in the plasmid backbone used for all constructions.

Integration was performed via a double crossover by the temperature sensitive plasmid, as described in detail by Millgaard et al. (2023). By growing the cells at 65 °C in SPY with kanamycin, the full plasmid is first integrated into one of the flanks, as the plasmid cannot replicate at such high temperatures. For the second recombineering event to occur, positive colonies are transferred to SPY media without antibiotic after which they are plated on kanamycin-free TSA. The second recombineering event can result in a return to WT cells (removal of the entire plasmid content) or in the removal of only the plasmid backbone and not the intended insert. Proper homologous recombineering was checked *via* colony PCR of non-fluorescent colonies using primers located outside the integration region. The whole list of primers used in this study is compiled in Table S1 (Supplementary Information).

Growth performance

Biomass growth was monitored by measuring the optical density at a wavelength of 600 nm (OD_{600}). Growth profiles were determined by growing the cells in a 24-well plate with controlled temperature at 60.0 ± 0.1 °C, and OD_{600} measurements every 10 min using a BioTek Epoch 2 microplate reader (Agilent, Santa Clara, USA). Maximum growth rate (μ_{max}) was calculated as the slope of the logarithm of OD_{600} against time during the exponential growth phase, which was determined as the period in which both parameters show a linear dependence.

Butanol production

P. thermoglucosidasius strains containing the full pathway were first grown on TSA plates. Preliminary butanol-producing assessment was performed in gas chromatography-mass spectrometry (GC-MS) headspace glass vials (total volume 20 mL) as follows: colonies were transferred to 2 mL TMM medium supplemented with glucose and YE and grown overnight at 60 °C with 200 rpm agitation in 24-deep well plates. Cells in stationary phase from this preculture were then spun down (3000 g, 5 min), resuspended in 2 mL fresh supplemented TMM with varying amounts of aTc (up to 0.5 µg/mL) to be used as an inducer before being transferred into the GC-MS vials. After 24 h, the vials containing the grown cells were rapidly quenched in an ice bath to stop growth and metabolism and sent for further analysis (described below).

For measuring biological butanol production, colonies from TSA plates were grown overnight in 30 mL TMM in shake flasks (total volume 250 mL). Inoculation for the production phase was performed aiming at an initial OD_{600} of 0.2 either in shake flasks with closed lid to minimize losses by evaporation of the desired alcohol, or in falcon tubes (total volume 50 mL) with varying amounts of liquid media to assess the influence of the air column. Induction with aTc was carried out when the cultures reached an OD_{600} of 0.5, marking the start of the exponential phase. Temperature for the production experiments was 60 °C with an agitation speed of 200 rpm. After 24 h, the flasks and/or tubes were rapidly quenched in an ice bath and sent for further analysis (described below). The yield of product per substrate consumed, $Y_{(P/S)}$, was calculated as the ratio between the final titre of butanol divided by the difference between initial and final glucose concentrations.

Microscopy imaging

Aliquots of 5 µL of grown cultures were transferred onto 1% (w/v) agarose pads located on a glass slide, and the sample was covered with a glass coverslip. Optical microscopy images were obtained through phase contrast microscopy, using a Leica DM4000 B microscope (Leica Microsystems, Wetzlar, Germany) with a 63x oil immersion objective.

Analytical methods

Butanol production was initially assessed by GC-MS on the headspace fraction of glass vials as previously described, using a GC-MS Bruker Scion 436 GC TQ (Scion Instruments, Goes, The Netherlands) equipped with a BP20 capillary column (30 m, internal diameter 0.25 mm, film thickness 0.25 mm) using helium as carrier. Liquid samples containing biomass were centrifuged at 10,000 rpm for 5 min, with the supernatant analysed for their content in sugars, organic acids and alcohols by high performance liquid chromatography (HPLC) using a Dionex Ultimate 3000 HPLC (Thermo Scientific, Waltham, USA) with an Aminex HPX87H ion exclusion column and 5 mM H_2SO_4 as eluent at a flow rate of 0.6 mL/min.

Results

Insertion of the thermophilic butanol production pathway in *P. thermoglucosidasius*

Several strategies were followed aiming to introduce the synthetic thermophilic pathway modelled by Loder et al. (2015). The initial strategy consisted of replacing the *ldh* gene (AOT13_05975) with the complete pathway consisting of six genes: this was initially attempted using pBUT01 which contains the full pathway in one operon without promoter. The result following this strategy was unsuccessful—different electroporation conditions were tested and transformation of the plasmid into the strain would not occur. A second strategy was designed, where the full pathway would be integrated into the same location in the chromosome although in two steps (using pBUT05 for the first insertion and pBUT07 for the remaining genes). The use of pBUT05 resulted in a successful integration of the first half of the pathway. For the second half, pBUT07 was successfully transformed into *P. thermoglucosidasius*, followed by the first crossover of the whole plasmid sequence. However, for all attempts the second crossover of pBUT07 resulted in the loop-out of the whole cassette, deeming integration of these genes unfeasible under the desired conditions. Given the apparent incompatibility of the whole pathway as a single operon, it was divided into two different operons located separately in the genome, following the strategy depicted in Fig. 2.

Plasmid pBUT17, containing genes *ter*, *bad* and *bdh* under control of an inducible Ptet promoter system, was utilised to integrate the second half of the pathway replacing the genes for acetone carboxylase (*acx*) subunits beta alpha and gamma (AOT13_09530, 09535, 09540). Considering that the two last enzymes involved in the pathway, Bad and Bdh, can also result in the production of ethanol starting from acetyl-CoA (Loder et al. 2015), the existing alcohol dehydrogenase system (*adh*) in *P. thermoglucosidasius* was knocked out with plasmid pJD45, to reduce the metabolic flux towards the two-carbon alcohol. The remaining genes (*thl*, *hbd*, *crt*) were integrated into the original desired position (replacing *ldh*) with pBUT28, albeit with an alternative *thl* gene from *Syntrophothermus lipocalidus* (Slip_0880) which was shown to provide a better kinetic performance when expressed in similar production pathways (unpublished data). The promoter for this operon was added after integration of the pathway genes, with several alternatives initially studied: three variants of a constitutive promoter (P10, P13 and P15, of decreasing expression levels of 7.8×10^4, 2.6×10^4, and 1.8×10^4 a.u., respectively, in terms of observed fluorescence when controlling the expression of sfGFP) (Pogrebnyakov et al. 2017), and a Ptet promoter without *tetR* as it was already present in the second operon (*tetR*-Ptet-*ter-bad-bdh*). The modified genome of the resulting strains with both operons integrated into the genome were named Btb-PX (where PX stands for the corresponding promoter of the first half of the pathway, being Ptet, P10, P13 or P15), as illustrated in Fig. 3.

Production of butanol with engineered *P. thermoglucosidasius* strains

Four strains were developed differing in the promoter of the operon containing the first half of the pathway. The preliminary assessment of butanol production in GC-MS vials provided the results shown in Fig. 4. For all strains, except the one with the weakest promoter (P15), butanol was observed even without the addition of the inducer. The strain containing the first operon under control of the weak P15 promoter showed similar results as the control, suggesting an almost unnoticeable expression of the first genes of the pathway. Highest butanol production was achieved with titres higher than 0.35 g/L when working under induced conditions with both operons under the control of the Ptet promoter, while cells with the operon containing the first genes (*thl-hbd-crt*) under the control of the constitutive P10 promoter (the highest constitutive promoter strength of those studied) under high induction levels showed similar production titres to BtB-Ptet using 0.1 aTc µg/mL.

Several production experiments were performed following various strategies in shake flasks, and no presence

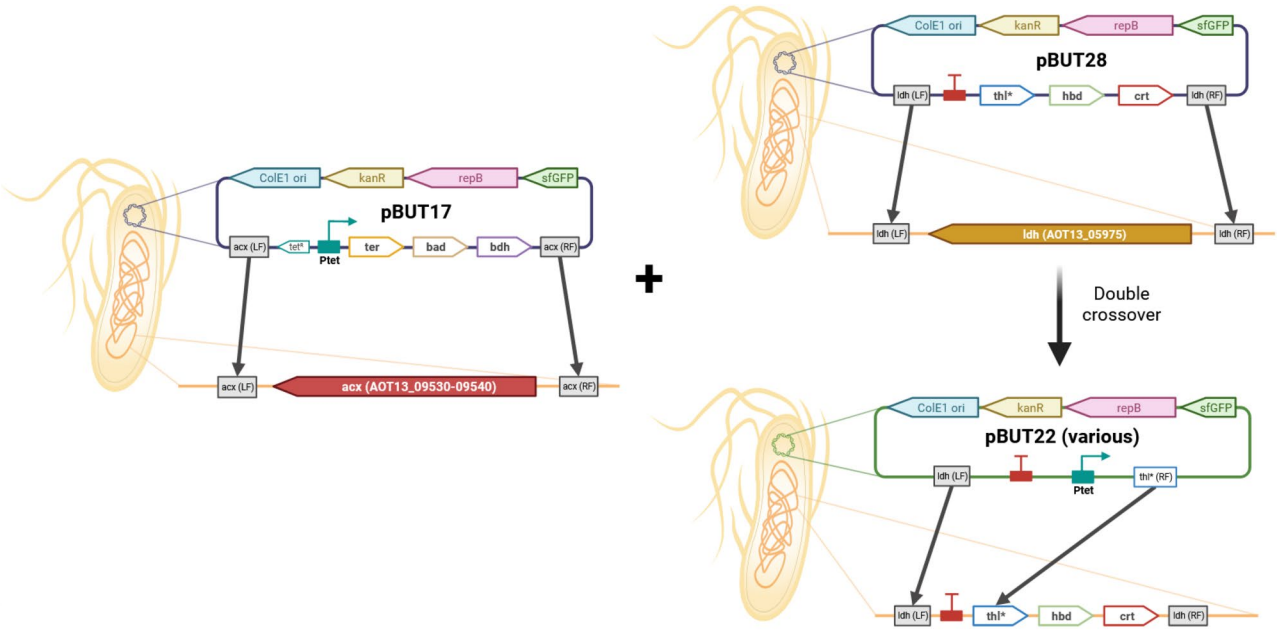

Fig. 2 Pathway insertion strategy into a Δ*adh P. thermoglucosidasius* strain. PlasmidpBUT17 was first used for insertion of the operon containing the second half of the pathway, along with a *tet*R-Ptet inducible promoter system, replacing *ldh*. Plasmid pBUT28 was used for insertion of the operon containing the first half, and plasmid pBUT22 for insertion of the promoter on this operon. Further variations of pBUT22 were utilised where the Ptet promoter was replaced by constitutive promoters P10, P13 and P15 stemming from the library described by Pogrebnyakov et al. (2017)

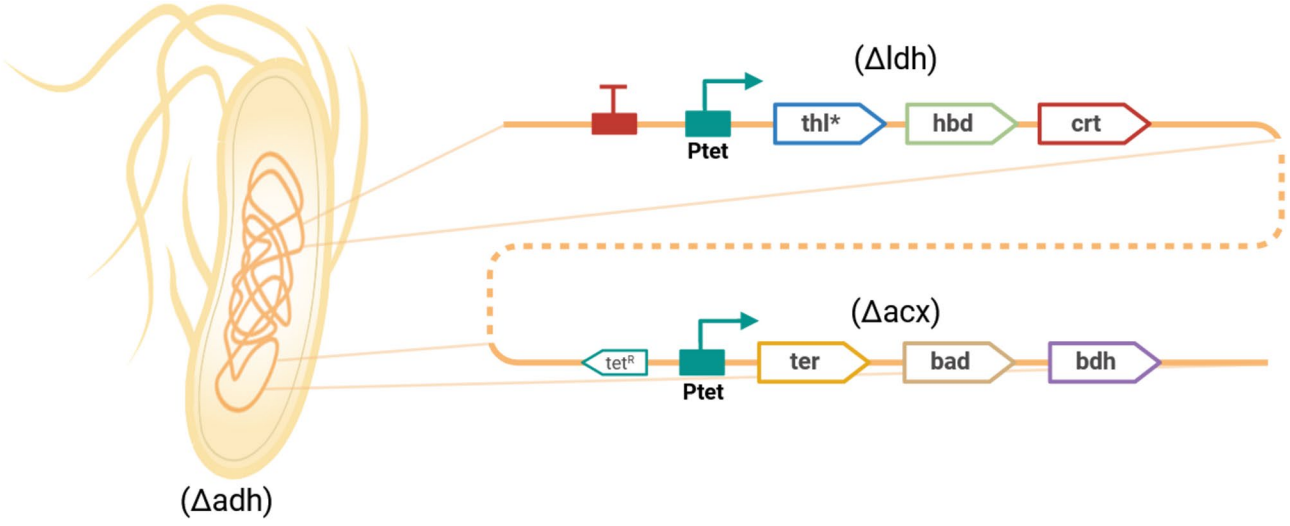

Fig. 3 *P. thermoglucosidasius* strain Btb-Ptet containing all six genes for the thermophilic production of butanol. Other versions of this strain were also tested in the present study where the Ptet promoter controlling the expression of the first operon containing *thl*, *hbd* and *crt* were replaced by constitutive promoters

of butanol was detected in any of them. HPLC analysis for Btb-Ptet cells grown both in shake flasks and in glass GC-MS vials showed varying performance outcomes. The cells grown in shake flask showed full glucose utilization and no apparent product formation, while those grown in glass vials showed an incomplete glucose consumption (1.83 ± 0.12 g/L glucose remaining after 24 h) and the formation of several by-products. These by-products included lactate (1.01 ± 0.07 g/L) and acetate (2.98 ± 0.13 g/L), which were observed in considerably lower quantities when grown in shake flask (up to 0.2 g/L lactate and 2 g/L acetate).

In order to assess the influence of aeration on the butanol production, various production experiments were

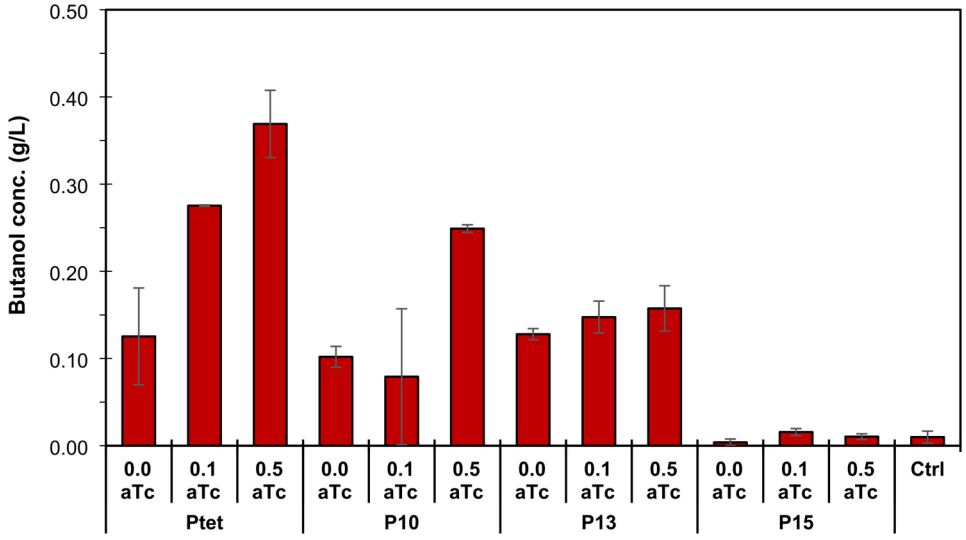

Fig. 4 Initial butanol production titres for strains containing different promoters controlling the transcription of the first operon (Ptet, P10, P13 and P15) using different induction levels (0.0, 0.1, 0.5 µg of aTc per mL of media). Control: Modified strain containing only the second operon (*ter-bad-bdh*) controlled by an inducible promoter, lacking the first operon (*thl-hbd-crt*) in its entirety

Table 2 Butanol production results with *P. thermoglucosidasius* Btb-Ptet cells grown in Falcon tubes with varying media volumes

Media volume (mL)	Air column volume (mL)	Butanol (g/L)	Glucose consumed (g/L)	$Y_{(P/S)}$ (%)
10	40	0.375 ± 0.018	4.72 ± 0.01	7.9 ± 0.3
20	30	0.161 ± 0.005	5.65 ± 0.01	2.8 ± 0.1
30	20	0.179 ± 0.000	5.36 ± 0.23	3.3 ± 0.1

run by growing the cells in falcon tubes (total volume 50 mL) with varying media volumes: 10, 20 and 30 mL. The results as analysed by HPLC are summarised in Table 2.

The butanol titres obtained for the experiment with the lowest media volume (and thus highest air-to-liquid ratio) were close to those obtained *via* GC-MS analysis, with a noticeable decrease in concentration as the air column decreased as well.

The length of the overnight culture prior to inoculation for the production experiments was found to be an important factor for subsequent butanol production. Some experiments carried out with a longer preculture, with cells staying longer in stationary phase, resulted in increased sporulation after induction, as can be seen through microscopy imaging (see Figure S1 in Supplementary Information). *P. thermoglucosidasius* is known to easily form spores when reaching stationary phase. Given the observed behaviour, the sporulation pathway knockout strategy developed by Millgaard et al. (2023) was applied, where plasmid pMM7 was utilised to obtain a *P. thermoglucosidasius* Btb-Ptet Δ*spo0A* strain expecting a better substrate uptake towards butanol and a more robust performance under industrial process conditions. This was however not the case; growth of Btb-Ptet Δ*spo0A* resulted in a lower butanol production of 0.268 ± 0.011 g/L.

Strains with Ptet and P10 guiding the expression of the first operon (*thl-hbd-crt*), with the highest butanol titres, had their growth performance assessed under no induction and high induction conditions (0.5 µg of aTc per mL of media). Growth curves for both experiments are shown on Fig. 5, while the corresponding μ_{max} values during exponential growth are compiled in Table 3.

Discussion

Considering the maximum theoretical yield of butanol (0.41 g butanol/g glucose, corresponding to the stoichiometric 1 mol butanol/1 mol glucose), the maximum titres obtained in the preliminary assessment (see Fig. 4) roughly correspond to a fermentation efficiency of 7% of the theoretical maximum. While not comparable to a typical *C. acetobutylicum* ABE fermentation process, where yields have been reported up to 0.35 g of butanol per g of glucose after appropriate engineering and adjustment of fermentation conditions (Nguyen et al. 2018), the observed butanol concentration already proves the feasibility of its production in the modified organism. This potential is expected to be improved with further metabolic engineering and under the right process conditions, allowing to maximise the yield from glucose or of other carbon sources which *P. thermoglucosidasius* can grow on, including for example acetate, xylose or glycerol (Mol et al. 2021).

The lack of butanol production in shake flask experiments suggest a negative effect caused by the presence of oxygen. Even though both experiments were performed using similar liquid-to-volume ratios, the enhanced

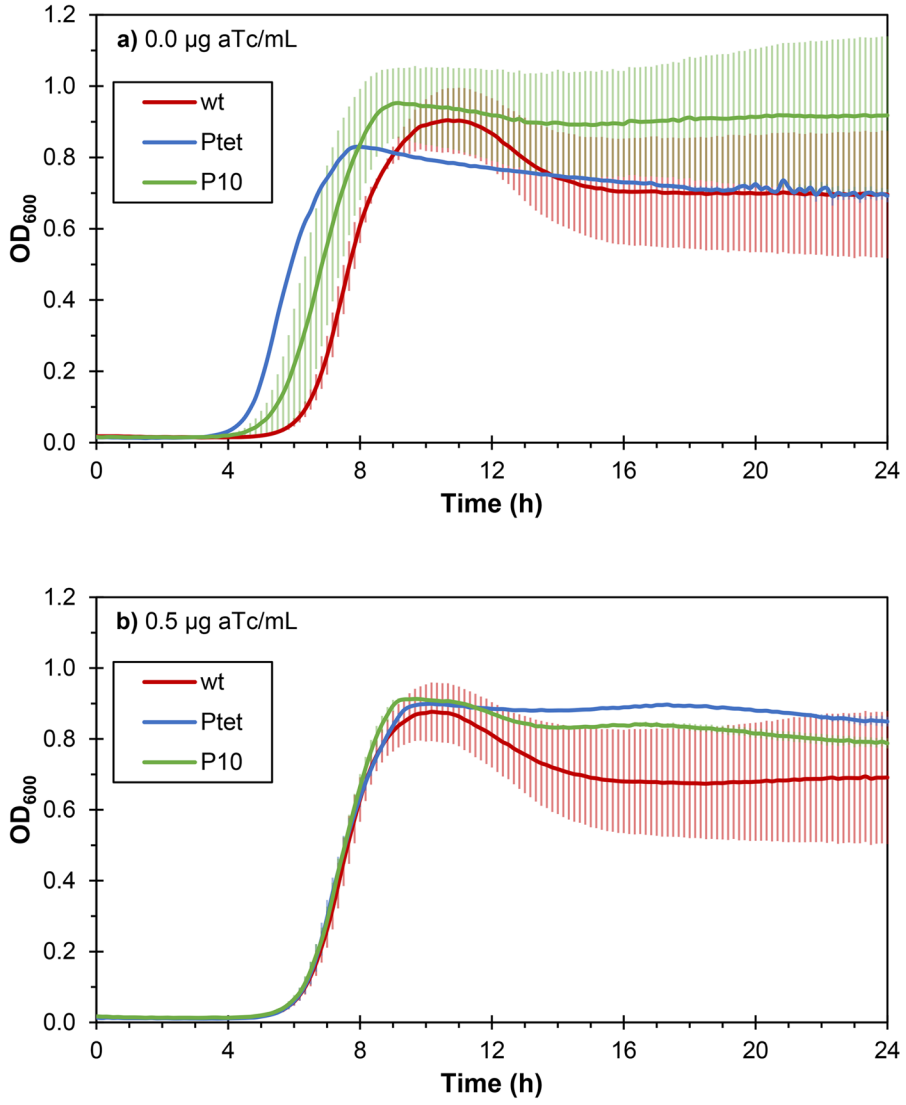

Fig. 5 Growth profiles of butanol-producing *P. thermoglucosidasius* Btb-PX strains with different promoters (Ptet in blue; P10 in green) controlling the operon containing the first half of the pathway, along with a wild type *P. thermoglucosidasius* DSM 2542 (red). Top (**a**): growth under no induction with aTc; bottom (**b**): growth with 0.5 µg of aTc per mL of media

Table 3 Maximal growth rates for every *P. thermoglucosidasius* Btb-PX strain along with a wild type *P. thermoglucosidasius* DSM 2542

Induction level (µg aTc/mL)	μ_{max} (h^{-1})		
	Btb-Ptet	Btb-P10	WT
0.0	1.62 ± 0.05	1.42 ± 0.11	1.44 ± 0.06
0.5	1.46 ± 0.03	1.43 ± 0.05	1.45 ± 0.04

shaking performance in shake flasks could provide a better aeration, affecting the oxygen transfer into the liquid phase. Fermentative by-products such as acetate or lactate in *Geobacillus* spp. are common in oxygen-limiting conditions, with these products acting as redox (case of lactate, as its production from pyruvate requires utilization of 2 NADH equivalents) or energy (case of acetate, as 2 ATP equivalents are obtained per molecule of acetate produced) sinks (Hussein et al. 2015). The production of lactate in a lactate dehydrogenase-knockout (*Δldh*) strain is noteworthy, though the titre observed in the WT strain was three-fold higher: 3.36 ± 0.07 g/L. The knockout of said gene contributed to decreasing the production of lactate but did not prevent it completely. This is likely due to the presence of promiscuous or unannotated enzymes that allowed for a by-passed production of the metabolite.

The lack of butanol production in shake-flasks, with efficient aeration and thus enhanced oxygen transfer to the fermentation broth, could be explained by the high demand for reducing cofactors (NADH) that the pathway requires, as seen in Fig. 1. Presence of oxygen may redirect flux to the tricarboxylic acid (TCA) cycle, from where reducing equivalents are recovered back to

NAD + due to respiration. Aerobic conditions are not suitable for the production of such a reduced product like butanol, with most native butanol producers such as *C. acetobutylicum* working under anaerobic conditions. As the aeration and thus oxygen availability and transfer between phases is limited in falcon tubes as opposed to shake flasks, this may explain the observed production of butanol on the former and not on the latter—the possibility of experiencing butanol losses due to evaporation was disregarded given the setup, using airtight lids when growing the cells in shake flasks and quenching them in ice baths for condensation of any possible leftover in the vapour phase.

P. thermoglucosidasius is a facultative anaerobe with proven enhanced growth rates in the presence of oxygen (Hussein et al. 2015). While full-anaerobic *P. thermoglucosidasius* growth has been shown (Mol et al. 2021), further investigation of the fermentation conditions needs to be performed to evaluate whether this would in turn provide higher product yields.

Removal of the sporulation behaviour resulted in a lower butanol production, an outcome contrary to previous approaches, where deletion of the *spo0A* gene in an ethanol-producing modified *P. thermoglucosidasius* was observed to provide ethanol titres matching those of the original strain (Atkinson et al. 2010). In *Bacillus subtilis*, species with a well-characterized sporulation pathway closely related to that of *P. thermoglucosidasius* (*spo0A* homology of approximately 80%) (Millgaard et al. 2023), this deletion was shown to result in a decrease in the production of riboflavin (Tännler et al. 2008). In the parent cell factory for the microorganism responsible for ABE fermentation (*C. acetobutylicum*), sporulation was however found to be coupled with the solventogenic phase where butanol is produced (Hu et al. 2011). Spo0A was found to be a central pathway regulator of said phase, and its suppression was tied to a decreased solvent production in the traditional ABE cell-factory, *C. acetobutylicum*. Given a large number of genes that are directly and indirectly regulated by Spo0A, it is likely that this regulation relation between sporulation through the initiator, Spo0A, and butanol production is still holding in the modified *P. thermoglucosidasius* strains, which could be related to the decrease in titre observed when it is suppressed. However, in order to fully ascertain the influence that sporulation (or lack thereof) has on the expression of the heterologous pathway, a further metabolic and transcriptomic study of its own is required and recommended for future work.

Overall, the three variants of the bacteria showed similar growth trends, with an almost identical performance under induced conditions. The presence of aTc showed no effect on the wild type *P. thermoglucosidasius* strain, revealing in both scenarios a similar lag phase length as well as equal growth rates with and without inducer. This result is in agreement to the work performed by Mol et al. (2022), where 0.5 µg aTc/mL was found to be the threshold for inhibited growth of the bacteria. Interestingly, a slightly longer lag phase was observed for the two modified strains, along with a lower μ_{max} for Btb-Ptet under induction conditions. Assuming the pathway genes under the control of the *tetR*-Ptet system are silent when uninduced, this could explain the apparent faster growth of Btb-Ptet over Btb-P10, which has the pathway for acetyl-CoA conversion to crotonyl-CoA constitutively expressed. As the main genetic difference apart from the inserted genes related to butanol production, the lack of *ldh* and *acx* operons could explain the difference in performance compared to the wild type.

All in all, the developed *P. thermoglucosidasius* butanol-producing strains establish a promising starting point to produce the four-carbon alcohol butanol under thermophilic conditions. The modified strain produced the desired alcohol butanol with concentrations up to 0.4 g/L, while its production was found to be heavily influenced by the presence of oxygen as the pathway is only effectively expressed under limited aerobic conditions. Further optimization of the pathway focused on increasing availability of reducing equivalents is expected to improve titres, rates and yields, or by performing a full-on analysis of possible metabolic bottlenecks by independently overexpressing each of the different enzymes involved in the butanol-production pathway.

Abbreviations

ABE	Acetone-butanol-ethanol
GC-MS	Gas chromatography-mass spectroscopy
HPLC	High-performance liquid chromatography
ISPR	In-situ product recovery
Kan	Kanamycin
LB	Lysogeny broth
SPY	Soy peptone-yeast
SSF	Simultaneous saccharification and fermentation
TCA	Tricarboxylic acid
TMM	Thermophile minimal medium
TSA	Trypticase soy agar
USER	Uracil-specific excision reagent
WT	Wild-type
YE	Yeast extract

Supplementary Information

The online version contains supplementary material available at https://doi.org/10.1186/s13568-025-01879-5.

Supplementary Material 1

Acknowledgements

The authors would like to thank Marie Millgaard for her contribution on the figures design, guidance on sporulation knockout strategies and assistance on microscopy imaging. Figures depicting gene insertion strategies were created with BioRender.com.

Author contributions
P.D.: Methodology, Formal analysis, Investigation, Writing—Original Draft, Visualization; I.P.: Conceptualization, Methodology, Validation, Investigation, Resources, Writing—Review & Editing; S.I.J.: Methodology, Resources, Writing—Review & Editing, Supervision; J.L.S.P.D.: Investigation, Resources; A.R.: Writing—Review & Editing, Supervision, Funding acquisition; A.T.N.: Writing—Review & Editing, Supervision, Project administration, Funding acquisition.

Funding information
This work was financially supported by the Independent Research Fund Denmark (grant number 1032-00448B), and by The Novo Nordisk Foundation through a grant to DTU Biosustain (Grant Number NNF20CC0035580), and we further acknowledge funding from the Villum Fonden (grant number 40986).

Data availability
Additional information as the list of primers or microscopy images can be found as Supplementary Information.

Declarations

Ethics approval and consent to participate
Not applicable.

Consent for publication
Not applicable.

Competing interests
The authors declare no competing interests.

Received: 16 December 2024 / Accepted: 16 April 2025
Published online: 13 May 2025

References

Abdel-Banat BMA, Hoshida H, Ano A, Nonklang S, Akada R (2010) High-temperature fermentation: How can processes for ethanol production at high temperatures become superior to the traditional process using mesophilic yeast? Appl Microbiol Biotechnol 85:861–867. https://doi.org/10.1007/s00253-009-2248-5

Anbarasan P, Baer ZC, Sreekumar S, Gross E, Binder JB, Blanch HW, Clark DS, Dean Toste F (2012) Integration of chemical catalysis with extractive fermentation to produce fuels. Nature 491:235–239. https://doi.org/10.1038/nature11594

Atkinson A, Cripps R, Eley K (2010) Sporulation-deficient thermophilic microorganisms for the production of ethanol

Atsumi S, Cann AF, Connor MR, Shen CR, Smith KM, Brynildsen MP, Chou KJY, Hanai T, Liao JC (2008) Metabolic engineering of *Escherichia coli* for 1-butanol production. Metab Eng 10:305–311. https://doi.org/10.1016/j.ymben.2007.08.003

Bhandiwad A, Shaw AJ, Guss A, Guseva A, Bahl H, Lynd LR (2014) Metabolic engineering of *Thermoanaerobacterium saccharolyticum* for n-butanol production. Metab Eng 21:17–25. https://doi.org/10.1016/j.ymben.2013.10.012

Breitkreuz K, Menne A, Kraft A (2014) New process for sustainable fuels and chemicals from bio-based alcohols and acetone. Biofuels Bioprod Biorefin 8:504–515. https://doi.org/10.1002/bbb.1484

Cripps RE, Eley K, Leak DJ, Rudd B, Taylor M, Todd M, Boakes S, Martin S, Atkinson T (2009) Metabolic engineering of *Geobacillus thermoglucosidasius* for high yield ethanol production. Metab Eng 11:398–408. https://doi.org/10.1016/j.ymben.2009.08.005

Doménech P, Pogrebnyakov I, Nielsen AT, Riisager A (2022) Catalytic production of long-chain hydrocarbons suitable for jet-fuel use from fermentation-derived oxygenates. Green Chem 24:3461–3474. https://doi.org/10.1039/D2GC00619G

Fletcher E, Pilizota T, Davies PR, McVey A, French CE (2016) Characterization of the effects of n-butanol on the cell envelope of *E. coli*. Appl Microbiol Biotechnol 100:9653–9659. https://doi.org/10.1007/s00253-016-7771-6

Fong JCN, Svenson CJ, Nakasugi K, Leong CTC, Bowman JP, Chen B, Glenn DR, Neilan BA, Rogers PL (2006) Isolation and characterization of two novel ethanol-tolerant facultative-anaerobic thermophilic bacteria strains from waste compost. Extremophiles 10:363–372. https://doi.org/10.1007/s00792-006-0507-2

Foulquier C, Rivière A, Heulot M, Dos Reis S, Perdu C, Girbal L, Pinault M, Dusséaux S, Yoo M, Soucaille P, Meynial-Salles I (2022) Molecular characterization of the missing electron pathways for butanol synthesis in *Clostridium acetobutylicum*. Nat Commun 13:4691. https://doi.org/10.1038/s41467-022-32269-1

Gabriëls D, Hernández WY, Sels BF, Van Der Voort P, Verberckmoes A (2015) Review of catalytic systems and thermodynamics for the Guerbet condensation reaction and challenges for biomass valorization. Catal Sci Technol 5:3876–3902. https://doi.org/10.1039/c5cy00359h

Gorter de Vries PJ, Mol V, Sonnenschein N, Jensen TØ, Nielsen AT (2024) Probing efficient microbial < scp > co $_2$ utilisation through metabolic and process modelling. Microb Biotechnol 17. https://doi.org/10.1111/1751-7915.14414

Hu S, Zheng H, Gu Y, Zhao J, Zhang W, Yang Y, Wang S, Zhao G, Yang S, Jiang W (2011) Comparative genomic and transcriptomic analysis revealed genetic characteristics related to solvent formation and xylose utilization in *Clostridium acetobutylicum* EA 2018. BMC Genomics 12:93. https://doi.org/10.1186/1471-2164-12-93

Hussein AH, Lisowska BK, Leak DJ (2015) The genus *Geobacillus* and their biotechnological potential. In: Advances in applied microbiology. Academic Press Inc., pp 1–48

Jiang Y, Guo D, Lu J, Dürre P, Dong W, Yan W, Zhang W, Ma J, Jiang M, Xin F (2018) Consolidated bioprocessing of butanol production from Xylan by a thermophilic and butanologenic *Thermoanaerobacterium* sp. M5. Biotechnol Biofuels 11:89. https://doi.org/10.1186/s13068-018-1092-1

Kananavičiūtė R, Čitavičius D (2015) Genetic engineering of *Geobacillus* spp. J Microbiol Methods 111:31–39. https://doi.org/10.1016/j.mimet.2015.02.002

Lau MSH, Sheng L, Zhang Y, Minton NP (2021) Development of a suite of tools for genome editing in *Parageobacillus thermoglucosidasius* and their use to identify the potential of a native plasmid in the generation of stable engineered strains. ACS Synth Biol 10:1739–1749. https://doi.org/10.1021/acssynbio.1c00138

Loder AJ, Zeldes BM, Garrison GD, Lipscomb GL, Adams MWW, Kelly RM (2015) Alcohol selectivity in a synthetic thermophilic *n*-Butanol pathway is driven by biocatalytic and thermostability characteristics of constituent enzymes. Appl Environ Microbiol 81:7187–7200. https://doi.org/10.1128/AEM.02028-15

Luyben WL (2008) Control of the heterogeneous azeotropic *n*-Butanol/water distillation system. Energy Fuels 22:4249–4258. https://doi.org/10.1021/ef8004064

Madika A, Spencer J, Lau MSH, Sheng L, Zhang Y, Minton NP (2022) pMTL60000: a modular plasmid vector series for *Parageobacillus thermoglucosidasius* strain engineering. J Microbiol Methods 202:106600. https://doi.org/10.1016/j.mimet.2022.106600

Millgaard M, Bidart GN, Pogrebnyakov I, Nielsen AT, Welner DH (2023) An improved integrative GFP-based vector for genetic engineering of *Parageobacillus thermoglucosidasius* facilitates the identification of a key sporulation regulator. AMB Express 13:44. https://doi.org/10.1186/s13568-023-01544-9

Mol V, Bennett M, Sánchez BJ, Lisowska BK, Herrgård MJ, Nielsen AT, Leak DJ, Sonnenschein N (2021) Genome-scale metabolic modeling of *P. thermoglucosidasius* NCIMB 11955 reveals metabolic bottlenecks in anaerobic metabolism. Metab Eng 65:123–134. https://doi.org/10.1016/j.ymben.2021.03.002

Mol V, Falkenberg KB, Will ÁDA, Pogrebnyakov I, Beck C, Skøttrup AL, Nielsen AT, Jensen SI (2022) From empirical to data-driven host selection: a broad-host-range expression platform to facilitate chassis screening (pre-print). bioRxiv. https://doi.org/10.1101/2022.08.09.503317

Nahreen S, Gupta RB (2013) Conversion of the acetone–butanol–ethanol (ABE) mixture to hydrocarbons by catalytic dehydration. Energy Fuels 27:2116–2125. https://doi.org/10.1021/ef302080n

Nawab S, Wang N, Ma X, Huo Y-X (2020) Genetic engineering of non-native hosts for 1-butanol production and its challenges: a review. Microb Cell Fact 19:79. https://doi.org/10.1186/s12934-020-01337-w

Ndaba B, Chiyanzu I, Marx S (2015) N-Butanol derived from biochemical and chemical routes: a review. Biotechnol Rep 8:1–9

Nguyen N-P-T, Raynaud C, Meynial-Salles I, Soucaille P (2018) Reviving the Weizmann process for commercial n-butanol production. Nat Commun 9:3682. https://doi.org/10.1038/s41467-018-05661-z

Pogrebnyakov I, Nielsen AT (2022) Methods and cells for production of volatile compounds

Pogrebnyakov I, Jendresen CB, Nielsen AT (2017) Genetic toolbox for controlled expression of functional proteins in *Geobacillus* spp. PLoS ONE 12:e0171313. https://doi.org/10.1371/journal.pone.0171313

Rumble JR (ed) (2022) Physical constants of organic compounds. CRC handbook of chemistry and physics (Internet Version), 103rd edn. CRC Press/Taylor & Francis, Boca Raton

Sheng L, Kovács K, Winzer K, Zhang Y, Minton NP (2017) Development and implementation of rapid metabolic engineering tools for chemical and fuel production in *Geobacillus thermoglucosidasius* NCIMB 11955. Biotechnol Biofuels 10:5. https://doi.org/10.1186/s13068-016-0692-x

Sheng L, Madika A, Lau MSH, Zhang Y, Minton NP (2023) Metabolic engineering for the production of acetoin and 2,3-butanediol at elevated temperature in *Parageobacillus thermoglucosidasius* NCIMB 11955. Front Bioeng Biotechnol. https://doi.org/10.3389/fbioe.2023.1191079

Swidah R, Ogunlabi O, Grant CM, Ashe MP (2018) n-Butanol production in *S. cerevisiae*: co-ordinate use of endogenous and exogenous pathways. Appl Microbiol Biotechnol 102:9857–9866. https://doi.org/10.1007/s00253-018-9305-x

Tännler S, Decasper S, Sauer U (2008) Maintenance metabolism and carbon fluxes in *Bacillus* species. Microb Cell Fact 7:19. https://doi.org/10.1186/1475-2859-7-19

Trindade WRdaS, dos Santos RG (2017) Review on the characteristics of butanol, its production and use as fuel in internal combustion engines. Renew Sustain Energy Rev 69:642–651. https://doi.org/10.1016/j.rser.2016.11.213

Weizmann C (1919) Production of acetone and alcohol by bacteriological processes

Xue C, Zhao J, Chen L, Yang ST, Bai F (2017) Recent advances and state-of-the-art strategies in strain and process engineering for Biobutanol production by *Clostridium acetobutylicum*. Biotechnol Adv 35:310–322

Zeldes BM, Straub CT, Otten JK, Adams MWW, Kelly RM (2018) A synthetic enzymatic pathway for extremely thermophilic acetone production based on the unexpectedly thermostable acetoacetate decarboxylase from *Clostridium acetobutylicum*. Biotechnol Bioeng 115:2951–2961. https://doi.org/10.1002/bit.26829

Zhou J, Lian J, Rao CV (2020) Metabolic engineering of *Parageobacillus thermoglucosidasius* for the efficient production of (2R, 3R)-butanediol. Appl Microbiol Biotechnol 104:4303–4311. https://doi.org/10.1007/s00253-020-10553-8

Publisher's note